Integrated protection and production in Viticulture
IOBC-WPRS Bulletin Vol. 105, 2014
pp. 137-148

Modelling of powdery mildew spread over a spatially heterogeneous growing grapevine

A. Calonnec[1], J. B. Burie[2], M. Langlais[3], Y. Mammeri[4]
[1]INRA, UMR1065 SAVE, 33883 Villenave d'Ornon, France; [2]Université de Bordeaux, ISVV, UMR SAVE, 33883 Villenave d'Ornon, France; [3]Université de Bordeaux, IMB, UMR 5251, 33076 Bordeaux, France; [4]LAMFA – CNRS UMR 7352, 80039 Amiens, France

Abstract: A PDE-ODE model was developed to describe the spread of powdery mildew on grapevine. The model was able to retrieve the main characteristics of the system: 1) a host growing during the whole season with time evolution in susceptibility, 2) a crop highly structured in rows with potential heterogeneities of plant growth and susceptibility within and between plots. These characteristics are modified by cultural management. Simulations were performed to test the effect of grapevine spatial heterogeneities, within and between plots, on the disease spread. Heterogeneities considered were the plant growth (vigour, earliness), susceptibility (susceptible vs resistant, treated vs untreated) and the spatial arrangements (patches vs rows). The main effect on disease reduction was obtained by arrangement in rows of susceptible and fully resistant plants.

Key words: pests, diseases, integrated control, heterogeneous plot

Introduction

To significantly reduce the use of fungicides, low-pesticide systems based on the development of innovative control methods, need to be developed. One of these control methods could rely on modification of plant growth and canopy architecture (Calonnec *et al.*, 2013). Spatial heterogeneity can be generated, at the plant, plot and landscape levels with changes over time. Setting up and implementing such alternatives in sustainable agriculture requires research to develop models able to explore hypotheses on their functioning and to test cropping systems that could be used to control and reduce disease spread.

Epidemiological models taking into account the crop growth and susceptibility are particularly important for the cultivated grapevine (*Vitis vinifera*), for which experiments are difficult to set up. Simulations allow generating plots or patches within plots, which differ in phenology, growth rate, crop management and training system for various climatic scenarii which can differently impact plant and pathogen growth. Grapevine show a high degree of spatial structure at the field level (culture in rows or individual vine, topped or not) and at individual plant level (various pruning types) exhibit rapid changes of susceptibility over time and is subjected to a high degree of human interference during its development. The powdery mildew/grapevine pathosystem, is highly susceptible and dependent on pesticides but we have evidence that variations within host populations do impact the disease incidence, severity or spread at different scales with direct links to leaf production (Calonnec *et al.*, 2009, Valdes-Gomez *et al.*, 2011). Training systems, favouring a high vegetative expression resulted also in higher levels of disease on bunches for different cultivars either moderately resistant (Gadoury *et al.*, 2001) or susceptible (Zahavi *et al.*, 2001). Those results on bunches were explained by a negative indirect effect of sun radiation on tissue susceptibility (Austin & Wilcox, 2011; Zahavi & Reuveni, 2012).

The epidemiological simulation models we devised coupling the grapevine growth with the dispersal and disease dynamics of the pathogen allow evaluating the ability of the host growth to modify fungal epidemics through the dynamic of organ production, their evolution of susceptibility and structure following climatic scenario or crop management. The first model we developed was a very detailed discrete mechanistic model describing the plant architecture and the development and dispersion of the pathogen accurately, at the plant scale (Calonnec *et al.*, 2008) with temperature and wind as forcing variables. The model confirmed observed experimental results about the effects of the rate of leaf emergence and of the number of leaves at flowering on the severity of the disease (Valdes-Gomez *et al*., 2011) and the crucial role of the date of primary contamination for disease severity (Calonnec *et al.*, 2006). At the plot scale the number of plants becomes however too large to describe each event in detail. An alternative approach is to use a continuous model for the leaf surface or for the density of leaves, i.e. the leaf surface area per unit of ground surface (leaf area index), with respect to its epidemiological state and its location in the plot. For a single plant, a system of ordinary differential equations (ODEs) of SLIRT type (Sensitive, Latent, Infectious, Removed, ontogenic resisTant) was proposed (Burie *et al.*, 2011). Host growth is handled as a logistic increase of the foliar surface before and after shoot topping. The ontogenic resistance of the leaves is taken into account. Using the output of the discrete model to calibrate the parameters of the SLIRT model, the host growth and the disease development was correctly reproduced with a short computing time. The ability of this mathematical model to retrieve the main dynamics of the disease for several vine growth scenarios was investigated (Burie *et al*., 2011). It underlines that strong variations of the dynamics of the disease due to an alteration of the synchronism between the disease and the production of susceptible organs depend more on the vine vigour than on climatic scenarios.

To extend the SLIRT model at the plot scale it is possible to couple a Reaction-Diffusion system at the plot scale with partial differential equations (PDEs) describing the spore dispersal mechanism to an ODEs model at the plant scale.

The objectives of this work were 1) to develop a coupled PDEs-ODEs model with a fine description of the spore dispersal process. The model includes biologically relevant parameters for powdery mildew development and grapevine growth taking into account the evolution of crop susceptibility (development age-related resistance) and agricultural practices such as shoot topping and fungicide applications and 2) to test, if this model is able to generate and explore the influence of host heterogeneities on epidemics spread control at the plot scale: heterogeneities within plot and between plots (e.g. phenology, vigour, plant resistance, spatial organization).

In the following, we present the model, then through numerical experiments we explore the evolution of the disease depending on grapevine heterogeneities of plant growth (vigour, earliness), and susceptibility (susceptible vs resistant, treated vs untreated), depending on canopy spatial arrangements (patches vs rows).

Material and methods

Model description

The unit considered for the description of the pathological state of the leaves surface is the leaf area index (LAI) defined as the leaf area in a one meter square section of ground area. The disease cycle is the following: susceptible leaves (denoted by S) inoculated with spores first become latent (L), then turn infectious (I) and produce spores during some infectious period after which they are removed (R) as they cannot be infected again. In addition,

susceptible leaves become resistant (T) to inoculation because of their age. The total LAI is denoted by N = S + L + I + R + T, the healthy LAI by H = S + T, and the diseased one by Di = N – H = L + I + R.

The disease has no significant impact on the plant growth. Thus, we assume the growth of the leaf area follows a logistic law with parameters $\alpha > 0$ and $k > 0$

$$\frac{d}{dt}N(x,t) = \alpha(x,t)N(x,t)\left(1 - \frac{N(x,t)}{k(x,t)}\right),$$

These coefficients may depend on the spatial location *x* according to the vigour of the vine and can be impacted by agricultural practices such as shoot topping. Shoot topping will first suppress part of the leaves and then induce a sudden change of the growth rate of the plant by enhancing secondary leaves development. Hence, we set

$$\alpha(x,t) = \begin{cases} \alpha_0(x)\ before\ shoot\ topping \\ \alpha_1(x)\ after\ shoot\ topping \end{cases}$$

$$k(x,t) = \begin{cases} k_0(x)\ before\ shoot\ topping \\ k_1(x)\ after\ shoot\ topping \end{cases}$$

The airborne spores densities are structured according to their dispersal mechanism leading to two ranges of dispersal: short ranged spores density (U_S) and long ranged one (U_L). The airborne spores are torn off from the colonies on the leaves by air turbulence and travel in the air according to a diffusion process. The distribution of the airborne spores *q(t,x)* emitted by a single lesion at the origin obeys a Gaussian density with a variance increasing linearly in time. Let denote *D*, the diffusion coefficient, the rate of increase of this variance. Spores are trapped on leaves and the time to trapping is assumed to be exponentially distributed with rate parameter δ. This leads to the multivariate probability distribution *Q* (the contact distribution) of trapped spores emitted from a single source over an infinite time span:

$$Q(x) = \int_0^{+\infty} \delta\, q(t,x)\, dt$$

$$q(t,x) = \frac{\exp(-\delta t)}{(2\pi t D)^{N/2}} \exp\left(-\sum_{i=1}^{2} (x_i)^2 / (2tD)\right).$$

Q(x), called Bessel distribution has been successfully fitted to experimental data for stripe rust (*Puccinia striiformis*) of wheat and downy mildew (*Peronospora farinosa*) of spinach. The order of the dispersal range is given by $\sigma = \sqrt{(D/\delta)}$. This modelling can be reformulated in terms of a PDE as follows, *q* is the fundamental solution of the diffusion equation

$$\partial_L q(x,t) - D\Delta q(x,t) + \delta q(x,t) = 0$$

where *q(0, x)* is the Dirac mass centered at the origin.

Once emitted from a colony, spores may remain trapped within the canopy and disperse at short range or escape the canopy and disperse at long range. Therefore, the concentration of airborne spores U_S and U_L obey the following advection-reaction-diffusion equations

$$\partial_t U_S(x,t) - \nabla.\left(D_S \nabla U_S(x,t)\right) + \delta_S U_S(x,t) = \gamma\ f\ I(x,t)$$
$$\partial_t U_L(x,t) - \nabla.\left(D_L \nabla U_L(x,t)\right) + V(x,t)\,\nabla U_L(x,t) + \delta_L U_L(x,t) = \gamma(1-f)I(x,t)$$

with *V* the velocity of the daily dominant wind on the spores above the canopy. Spores are produced by unit of infectious leaves area *I(x,t)* at rate $\gamma > 0$. Each emitted spore has a probability *f* in [0,1] to be short-range dispersed and thus a probability *(1 − f)* to be long-range dispersed (escaping the canopy). The escape probability depends on the total leave density *N* as one expects the spore dispersal range to be reduced when the LAI is larger. Airborne spores land on plants at short range and long-range deposition rates $\delta_S > 0$ and $\delta_L > 0$, and infect the leaves with a specific efficiency e_S, e_L. Long-range spores have smaller infection efficiency than the short-range ones consecutive to their longer exposition to UV radiation during their airborne transportation (Willocquet *et al.*, 1996), i.e. $0 < e_L < e_S$.

This leads to the following compartmental submodel for LAIs, defined by a system of ODEs parameterized by *x* in some spatial domain Ω,

$$\frac{d}{dt}S(x,t) = -a\left(e_s\delta_s U_S(x,t) + e_L\delta_L U_L(x,t)\right)\frac{S(x,t)}{N(x,t)} + \alpha N(x,t)\left(1 - \frac{N(x,t)}{k}\right) - \frac{1}{m}S(x,t)$$
$$\frac{d}{dt}L(x,t) = a\left(e_s\delta_s U_S(x,t) + e_L\delta_L U_L(x,t)\right)\frac{S(x,t)}{N(x,t)} - \frac{1}{j}L(x,t)$$
$$\frac{d}{dt}I(x,t) = \frac{1}{j}L(x,t) - \frac{1}{i}I(x,t)$$
$$\frac{d}{dt}R(x,t) = \frac{1}{i}I(x,t)$$
$$\frac{d}{dt}T(x,t) = \frac{1}{m}S(x,t)$$

Parameter *a* is defined as the average size of infected area created by a single spore (i.e. the size of a colony), and *m* as a mean period of susceptibility of the foliar surface to the disease (ontogenic resistance). The colonies do not produce spores during a mean latent period *j* then sporulate during a mean infectious period *i*.

This model system is supplemented with nonnegative initial conditions S_0, L_0, I_0, R_0, T_0 and US_0, UL_0. The row structure of the plot is handled by defining for each row a subdomain Ω_i of Ω where *N(t,x) = S(t,x) = L(t,x) = I(t,x) = R(t,x) = T(t,x) = 0* for all *t* when *x* is not in Ω_i between rows. Moreover, within each row, subdomains $\Omega_{i,j}$ of Ω_i can be defined for which plant growth related functions α and k are piecewise constant corresponding to potential vigour heterogeneities. As a consequence, LAIs are discontinuous functions of space.

Diffusion coefficients D_S, D_L may also depend on *N*, in which case, they are spatially discontinuous. At shoot topping (removal of leaves) a new simulation starts with another set of initial conditions derived from the result of the previous one.

Parameter calibration

The model parameters are either taken from the literature (D_S, D_L, δ_S, δ_L, *i*, *j*, *m*) or estimated at the plant scale from the outputs of the architectural model (α, k, γ). To measure the sensitivity of the epidemic behaviour to some parameter variations, we allowed parameters such as the proportion *(f)* (proportion of short distance dispersal spores) and the infection efficiency of spores dispersed at short (e_s) vs long distance (e_L), to vary. The greater diseased

area and spread on the plot is observed for f=0.8. Best matching values for (f,e_S,e_L) were selected based on the results of data of disease progression (Calonnec *et al*., 2009).

Dispersal related parameters were set using biologically relevant magnitudes as described above (Van den Bosch *et al.*, 1988; Zawolek & Zadoks, 1992). We made the assumption that the average time for the airborne spores to fall over the plant is half an hour and the short distance dispersal coefficients is set so that the spores disperse within the vine stock.

Parameters values are summarized in Table 1.

Table 1. Parameters definition and value used for simulations

Type	Parameter Abbreviation	Name	Simulation	Value
parameters linked to the dispersion	δ_S	spore deposition rate at short distance	all	50 day^{-1}
	δ_L	spore deposition rate at long distance	all	50 day^{-1}
	σs	standard deviation of short distance fallen spores	all	2 m
	σ_L	standard deviation of long distance fallen spores	all	20 m
	D_s	diffusion coefficient at short distance	all	200 m^2 day^{-1}
	D_L	diffusion coefficient at long distance	all	20000 m^2 day^{-1}
	f	probability of short-range dispersion	all	0.8
parameters linked to the pathogen	γ	rate of spore production	Before topping vig 1	2655 day^{-1}
			After topping vig 1	2033 day^{-1}
			Before topping vig 0.2	2263 day^{-1}
			After topping vig 0.2	1794 day^{-1}
	i	infectious period	all	10 days
	j	sporulation period	all	10 days
	m	latence period	all	10 days
	e_S	spore infection efficiency for short distance dispersed	all	0.07%
	e_L	spore infection efficiency for long distance dispersed	Resistant variety	1/100 of susceptible variety
			Fungicide treatment	0 during 10 days
			Susceptible variety	0.06%
			Resistant variety	1/100 of susceptible variety
			Fungicide treatment	0 during 10 days
parameters linked to the plant	α	plant growth rate	Before topping	0.1476 day^{-1}
			After topping vig 1	0.0416 day^{-1}
			After topping vig 0.2	0.0037 day^{-1}
	k	plant growth capacity	Before topping vig 1	25 701 cm^2/vinestock
			After topping vig 1	171 230 cm^2/vinestock
			After topping vig 0.2	181 880 cm^2/vinestock

The architectural model (A) describing the growth of one plant and the propagation of the pathogen within this plant and its porting on the Open Alea platform (Calonnec *et al*., 2008; Pradal *et al.*, 2008) provides us daily data for the density of susceptible (S_A), latent (L_A), infectious (I_A), removed (R_A) and ontogenic resistant leaves (age more than m days) (T_A) at the plant scale. At shoot topping, part of each compartment is removed and the state of each compartment and the growth parameters are updated. The amount of spores propagating inside the plant as well as of those outgoing from the plant is also available, giving $U_{S;A}$, $U_{L;A}$. From the amount of diseased tissue (I_A) and the amount of spore produced (g_A), the spore production is calibrated (g) and the average rate of spore production (γ) is assessed.

The time evolution of the total leaf surface area from the architectural model is fitted to a logistic law to estimate α and k.

A least square method is used to fit data and minimize the relative square difference J, defined as the sum of squared residuals divided by the sum of squared outputs.

Numerical simulations at the plot scale

Simulations are performed with a plot including 50 rows of width 0.5 m and length 98.4 m with 1.5 m inter-rows. The number of plants per row is 123, making a total of 6150 plants. One vine stock covers a soil surface area of 0.4 m^2.

Simulations procedure is as follows:

– Simulations start at day of primary inoculation, with a given LAI of total, susceptible, latent and ontogenic resistant leaves provided by the architectural model (climatic data of 2004). The initial density of infectious and removed leaves and the initial concentration of spores are zero.

– Parameter estimations of plant growth and spore production rate are determined. This estimation is made before and after topping separately and the amount of each type of tissue is updated after shoot topping taking into account the amount of each type of tissue removed by the cultural management. The day of shoot topping is set at day 173, 10 days after flowering (day 163) according to this climatic data scenario. With these parameters, we simulate the epidemic for the whole season.

– Numerical simulations are performed on the plot.

Crop heterogeneity simulations

Simulations are performed to test the influence of heterogeneities of crop growth (vigour, earliness), of crop susceptibility (susceptible vs. resistant) on the disease spread depending on the canopy spatial arrangements (patches vs. rows) combined with or without fungicide treatments (Table 2).

Effect of plant-pathogen synchronism on disease spread. In these simulations we measure the effect on disease spread of a shift in phenology (delay of budbreak) between two adjacent plots depending on the location of primary infection (on the early bud break plot or on the late bud break plot). A plot made of vigor 1 plants is separated into two parts: one part (block 1) for which plant growth start at day 119 (early bud break) and one part (block 2) for which plant growth is delayed by 10 days (late bud break). Delayed growth is taken into account in the model by imposing $\alpha = 0$ for 9 days. The infection begins at the center of one or the other part (Simulation 1a, 1b, Table 2).

Effect of plant growth or plant susceptibility heterogeneities on disease spread. In these simulations we compare the epidemic spread on a plot with heterogeneities in plant growth (vigour 1 or 0.2) or plant susceptibility (susceptible vs. resistant) depending on the date of inoculation and on the structure of the canopy (heterogeneities arranged in patches or rows) (Simulation 2a, 2b 3a, 3b Table 2).

Table 2. Conditions of the simulations performed

Hypotheses tested	simulation number	plant distribution/type*	treatment	budbreak date	inoculation location
Effect of plant-pathogen synchronism on disease spread	1a	patches 1,3 /early budbreak patches 2,4 /late budbreak 	No	118 128	center block 1
	1b	patches 1,3 /early budbreak patches 2,4 /late budbreak 	No	118 128	center block 2
Effect of plant growth heterogeneities on disease spread	2a	patches 2,3 /vigour 0.2 patches 1,4 /vigour 1 	No	118	center plot
	2b	alternate rows/vigour 1 /vigour 0.2 	No	118	center plot
Effect of heterogeneities of plant susceptibility on disease spread	3a	patches 2,3 /resistant patches 1,4 /susceptible 	No	118	center plot
	3b	alternate rows/susceptible /resistant 	No	118	center plot
Effect of disease control	4a	whole plot vigour 1 	fungicide at flowering	118	center plot
	4b	whole plot vigour 1 	fungicide at shoot topping	118	center plot

*the whole plot (50 rows x 123 vines) is shared in two blocks of 25 rows x 123 vines (I and II) or 4 patches of 25 rows x 61 vines (1, 2, 3, 4)
black point indicate the position of the initial inoculation

Effect of disease control. Disease control impact is tested by applying a fungicide treatment at flowering or topping (Simulations 4a, 4b, Table 2). Fungicide treatments are taken into account in the model by imposing $e_S = e_L = 0$ for 10 days.

Results

Effect of plant-pathogen synchronism on disease spread

On a plot divided in two blocks with different bud break dates, dynamics of epidemics depends on when and where the primary inoculum started. When the disease started on the early bud break part, it spread quickly with a high level of disease and propagated on the late bud break part but at a lower level (block 1 inoculated, Figure 1A). The total amount of disease on the whole plot is higher than the disease amount computed on a homogenous plot with either early or late bud break. When the disease started early on the late bud break part (block 2 inoculated, Figure 1B), the disease was mainly restrained on the inoculated block and this level was low, the ontogenic resistance being high on the early bud break part when the disease reached block 1. The whole plot was less diseased than if the disease had started on the early bud break block. Therefore, variability of crop phenology between plots can create higher or lower level of epidemics and spread depending on the location of the disease initiation. When the heterogenous plot was inoculated on the late bud break part (1b), disease was decreased of 79% at shoot topping and 64% at day 220 compared to the homogenous plots, and when the disease started on the early bud break part (1a), the disease was decreased of 44% at shoot topping and 31% at day 220, with a lower level of disease around the focus compared to the homogenous plot.

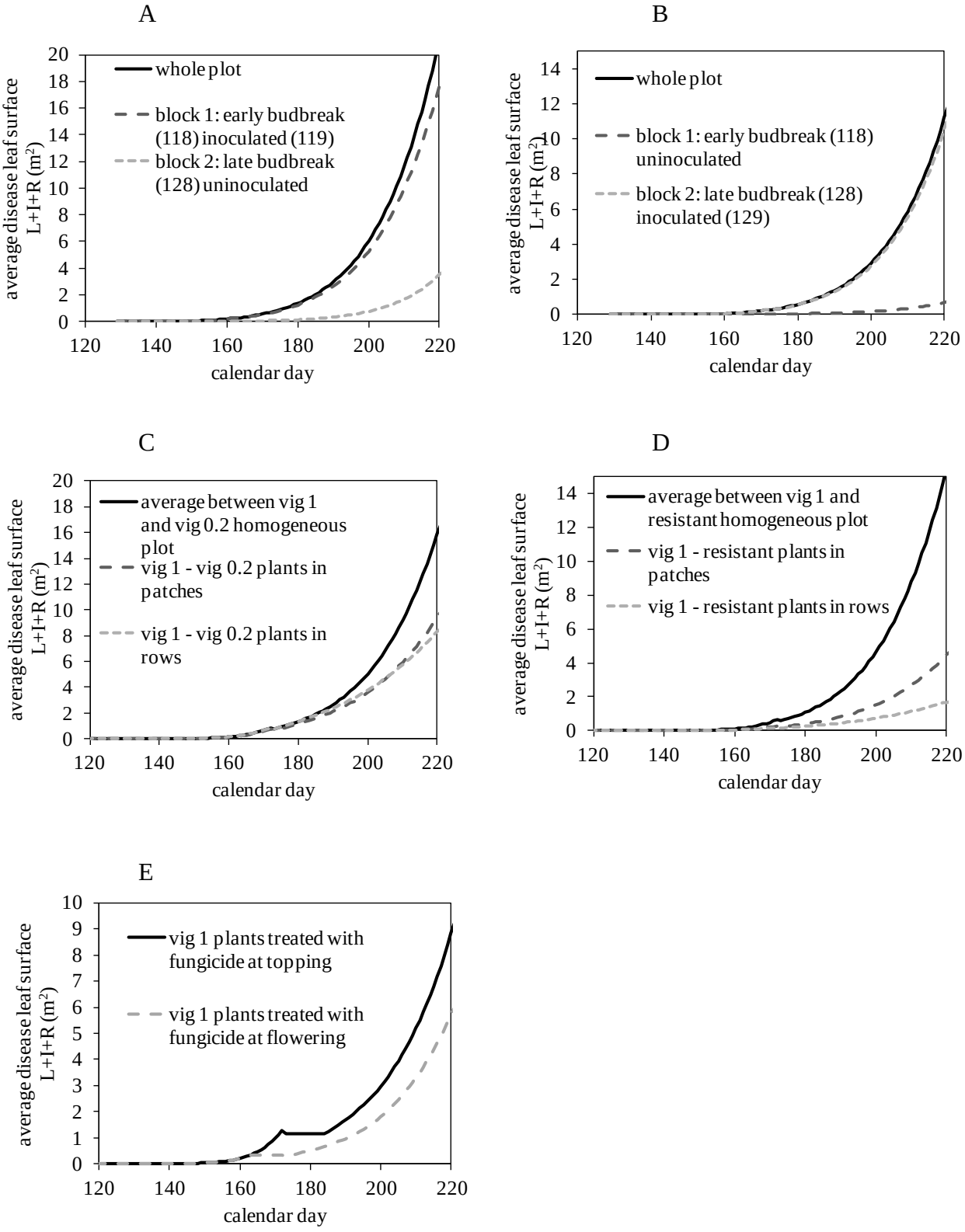

Figure 1. Temporal evolution of the total diseased surface area simulated by the PDE-ODE model, for conditions described in Table 1: simulations 1a (A), 1b (B), 2a and 2b (C), 3a and 3b (D), 4a and 4b (E).

Effect of plant growth or plant susceptibility heterogeneities on disease spread

For a plot equally mixed with plants of different vigour (1 and 0.2), the total amount of disease at the end of the season was decreased for both patterns of heterogeneities, rows (47%) or patches (40%), compared with the arithmetic mean of the amounts of disease observed on vigour 1 and 0.2 homogenous plots (Figure 1C). The difference between the two crop management designs was however only significant late in the season (from day 210). Disease spread was smaller when vigour heterogeneity was distributed in rows rather than in patches, at least for high vigour.

Similarly, for a plot mixing resistant and vigour 1, in both cases (patches and rows) the disease amount was strongly reduced (Figure 1D) compared with the mean of corresponding homogeneous plots. Again the disease reduction effect was higher when plants are mixed in rows (71% disease reduction at shoot topping and 89% at day 220) than in patches (58% disease reduction at shoot topping and 70% at day 220) both for amount and spread.

To conclude with the effect of crop managements on disease reduction, the hierarchy of their efficiencies differs at shoot topping and at the end of the season. At shoot topping we can order disease reduction as: plant-pathogen synchronism with inoculation in late bud break part (79% disease reduction) > heterogeneities for susceptibility in rows (71%) > heterogeneities for susceptibility in patches (58%) > plant-pathogen synchronism with inoculation in early bud break part (44%) > heterogeneities for growth in patches (12%) > heterogeneities for growth in rows (disease increase +3%). At the end of the season, it becomes: heterogeneities for susceptibility in rows (89%) > heterogeneities for susceptibility in patches (70%) > plant-pathogen synchronism with inoculation in late bud break part (64%) > heterogeneities for growth in rows (47%) > heterogeneities for growth in patches (40%) > plant-pathogen synchronism with inoculation in early bud break part (31%).

Effect of disease control measures

A fungicide treatment is mimicked by enforcing an infection efficiency equal to zero during 10 days. One application of fungicide at flowering reduces the diseased surface of 69% at shoot topping and 81% at day 220, whereas when the fungicide was applied at shoot topping the disease reduction was only 71% at the end of the season compared to an untreated plot (Figure 1E). Even if the decrease of diseased foliar area is significant around the primary focus of infection, conversely the spread of the disease on the plot is only slightly reduced by the fungicide.

Discussion

The PDE-ODE model was able to simulate a powdery mildew epidemic during a whole season at the scale of an entire grapevine plot, including management practices such as row layout, shoot topping, varietal mixtures and fungicide applications. Simulations showed that variations of crop growth, phenology and susceptibility have an effect not only at the vine scale as observed before, but also a major effect at the plot scale. Showing that this effect can be investigated by modeling, gives us the possibilities to explore more designs of crop management. The model in its actual form allowed generating spatial heterogeneities in terms of plant and crop structure and plant susceptibility inducing various effects on disease dynamics and propagations. The heterogeneities simulated in this work aim at exploring practical issues that regularly come from practitioners: 1) Do heterogeneities of phenology such as the one observed between adjoined varieties/plots can favor the disease? 2) Can the management of plant vigour help having a better control of the disease? 3) Can varietal

mixture with various levels of resistance reduce the disease spread? 4) What is the better timing to apply a fungicide?

We tested some scenarios and studied the effect of the variation of some key parameters that seem to be consistent with field epidemics and theoretical studies. It is difficult to validate whether levels in terms of diseased surface are consistent with biological data at the plot scale. Indeed, such data including disease and plant growth are impossible to acquire at this scale and can only be approximated visually or by different censors. The PDE-ODE model does not neither allow us to extract the frequency of diseased leaves which is a data easy to collect at the field scale and which could help us to verify the relationship between two levels of spatial hierarchy (leaves and vines) recognized as the signature of dispersion of a pathogen (Hughes *et al.*, 1997, McRoberts *et al.*, 2003). However, expressing the model output in terms of diseased vines (rather than diseased area), help us to calibrate parameters of dispersion such as *f* and parameters of spore infection efficiency (e_s-e_L). The value of *f* (0.8) for the proportion of spores short range dispersal gives optimal disease spread consistent with the field data of the frequency of diseased vines and numerical simulations obtained for different plant pathogen systems (Zawolek and Zadoks, 1992).

Results showed that desynchronisation between plant phenology and pathogen cycle can have a strong effect early in the season. The simulations performed with plots of various budbreak dates highlight that the intensity of the disease reduction depends on location of primary inoculum in relation to crop phenology: the disease can be decreased from 44 to 79% at shoot topping and from 31 to 64% at the end of the season, compared to epidemics spreading on a homogenous plot. Introducing heterogeneities in phenology either through varieties, plantation age, pruning date, temperature variation, may have an effect on disease reduction which can be explained by the rapid evolution of tissue resistance combined with the dispersion range used.

Mixing plants with various levels of vigours differing by the production of secondary leaves after shoot topping will however have moderate and late effects on disease. With this type of plant mixture the level of inoculum decreases after shoot topping (fewer spores are produced on low vigorous plants). At this time the epidemic focus is already strong enough for the disease to invade vigorous plants even if the level of spores emitted on low vigour plants drops. On the contrary, combining highly vigorous plants with almost totally resistant plants will have a major effect on disease spread very early in the season cycle. In this case, the effect of disease reduction is a combination of barrier effect (spores are lost on resistant rows or patches) and of a decrease of the inoculum production. The effect of varietal mixture on disease reduction is well known in phytopathology Wolfe, 1985, but only few examples exist on perennial crops such as apple trees (Bousset *et al.*, 1997; Didelot *et al.*, 2007) and grapevine (Didelot *et al.*, 2007; Matasci *et al.*, 2006). In these examples, the resistant varieties were not fully resistant, arranged in rows and the effects were only partial. On Apple/Apple scab the effect on disease reduction was higher when limited fungicide treatments were used.

The size and the distribution of resistant patches at the landscape level for disease reduction or for the sustainability of resistant varieties are of growing interest in phytopathology. The efficacy of spatial disease management strategies appears to be higher when heterogeneities in host population increase at a finer scale (Skelsey *et al.*, 2010). What we observed about the increased disease reduction, when plant heterogeneities are distributed in rows rather than in patches is consistent with these results. In another model of fungal disease combining short distance dispersal with stochastic long range dispersal, it was showed that epidemic speed was best reduced for either the finest grain of patches (mixing resistant and susceptible plants) or the coarsest grain of patches (remote susceptible plots scattered

among resistant plots) (Sapoukhina *et al.*, 2010). Intermediate heterogeneous patterns, like rows were less efficient.

Finally, in our preliminary approach of simulations with fungicide use, we showed that one fungicide applied early at flowering can significantly reduce (81%) diseased area at the end of the season by delaying the epidemic onset. More importantly it can maintain a low level of disease at a key period when the dispersion of the pathogen from leaves to bunches can be detrimental. Fungicide action was taken into account in the model by setting the spores contamination efficiencies at 0 at various times in the season and during some given period of time. Other mechanisms could be used as setting the production of spores to 0 during some period of time which could fit with various fungicide mechanisms on powdery mildew (Delière *et al.*, 2010). Other combinations of date, numbers of fungicide treatments, effects on pathogen cycle (on infection efficiency or sporulation) and localized application will be performed.

Acknowledgments

This work was funded by the Agence Nationale de la Recherche (ANR): project ARCHIDEMIO grant ANR-08-STRA-04

References

Austin, C. N., Wilcox, W. F. 2011: Effects of fruit-zone leaf removal, training systems, and irrigation on the development of grapevine powdery mildew. Am. J. Enol. Vitic. 62(2): 193-198.

Bousset, L., Blaise, P., Kellerhals, M., Gessler, C. 1997: Mixtures of apple cultivars in orchards: effect on the scab epidemics. Bulletin OILB-SROP 20(9): 42-48.

Burie, J. B., Langlais, M., Calonnec, A. 2011: Switching from a mechanistic model to a continuous model to study at different scales the effect of vine growth on the dynamic of a powdery mildew epidemic. Annals of Botany 107(5): 885-895.

Calonnec, A., Burie, J.-B., Langlais, M., Guyader, S., Saint-Jean, S., Sache, I., Tivoli, B. 2013: Impacts of plant growth and architecture on pathogen processes and their consequences for epidemic behaviour. European Journal of Plant Pathology 135: 479-497.

Calonnec, A., Cartolaro, P., Chadoeuf, J. 2009: Highlighting Features of Spatiotemporal Spread of Powdery Mildew Epidemics in the Vineyard Using Statistical Modeling on Field Experimental Data. Phytopathology 99(4): 411-422.

Calonnec, A., Cartolaro, P., Deliere, L., Chadoeuf, J. 2006: Powdery mildew on grapevine: the date of primary contamination affects disease development on leaves and damage on grape. Bulletin OILB-SROP 29(11): 67-73.

Calonnec, A., Cartolaro, P., Naulin, J. M., Bailey, D., Langlais, M. 2008: A host-pathogen simulation model: powdery mildew of grapevine. Plant Pathology 57: 493-508.

Delière, L., Miclot, A. S., Rey, P., Calonnec, A. 2010: Efficacy of fungicides with various modes of action in controlling the early stages of an *Erysiphe necator*-induced epidemic. Pest Management Science 66: 1367-1373.

Didelot, F., Brun, L., Parisi, L. 2007: Effects of cultivar mixtures on scab control in apple orchards. Plant Pathology 56(6): 1014-1022.

Gadoury, D. M., Seem, R. C., Pearson, R. C., Wilcox, W. F., Dunst, R. M. 2001: Effects of powdery mildew on vine growth, yield, and quality of concord grapes. Plant Dis. 85(2): 137-140.

Hughes, G., McRoberts, N., Madden, L. V., Gottwald, T. R. 1997: Relationships between disease incidence at two levels in a spatial hierarchy. Phytopathology 87(5): 542-550.

Matasci, C., Jermini, M., Gobbin, D., Rosselli, N., Gessler, C. 2006: Influence of cultivar mixtures on grapevine Downy mildew epidemic. In: Proc. 5th Int. workshop on Grapevine downy and powdery mildew. San Michele all'Adige, Italy, 18-23 June, 2006 (eds. Pertot, I., Gessler, C., Gadoury, D. M., Gubler, W. D., Kassemeyer, H.-H. & Magarey, P.).

McRoberts, N., Hughes, G., Madden, L. V. 2003: The theoretical basis and practical application of relationships between different disease intensity measurements in plants. Annals of Applied Biology 142(2): 191-211.

Pradal, C., Dufour-Kowalski, S., Boudon, F., Fournier, C., Godin, C. 2008: OpenAlea: A visual programming and component-based software platform for plant modeling. Functional Plant Biology 35(9-10): 751-760.

Sapoukhina, N., Tyutyunov, Y., Sache, I., Arditi, R. 2010: Spatially mixed crops to control the stratified dispersal of airborne fungal diseases. Ecological Modelling 221(23): 2793-2800.

Skelsey, P., Rossing, W., Kessel, G., van der Werf, W. 2010: Invasion of *Phytophthora infestans* at the landscape level: how do spatial scale and wheather modulate the consequences of spatial heterogeneity in host resistance? Phytopathology 100: 1146-1161.

Valdes-Gomez, H., Gary, C., Cartolaro, P., Lolas-Caneo, M., Calonnec, A. 2011: Powdery mildew development is positively influenced by grapevine vegetative growth induced by different soil management strategies. Crop Protection 30: 1168-1177.

Van den Bosch, F., Zadoks, J. C., Metz, J. A. J. 1988: Focus expansion in plant disease. I: The constant rate of focus expansion. Phytopathology 78: 54-58.

Willocquet, L., Colombet, D., Rougier, M., Fargues, J., Clerjeau, M. 1996: Effects of radiation, especially ultraviolet B, on conidial germination and mycelial growth of grape powdery mildew. European Journal of Plant Pathology 102(5): 441-449.

Wolfe, M. S. 1985: The current status and prospects of multiline cultivars and variety mixtures for disease resistance. Annual Review of Phytopathology 23(1): 251-273.

Zahavi, T., Reuveni, M. 2012: Effect of grapevine training systems on susceptibility of berries to infection by *Erysiphe necator*. European Journal of Plant Pathology DOI 10.1007/s10658-012-9938-z.

Zahavi, T., Reuveni, M., Scheglov, D., Lavee, S. 2001: Effect of grapevine training systems on development of powdery mildew. European Journal of Plant Pathology 107: 495-501.

Zawolek, M., Zadoks, J. C. 1992: Studies in focus development: An optimum for the dual dispersal of plant pathogens. Phytopathology 82(11): 1288-1297.